RESEARCH PAPER

PCCP
www.rsc.org/pccp

Effects of ultrasound on the microenvironment in reverse micelles and synthesis of nanorods and nanofibers

Jianling Zhang, Buxing Han,* Dongxia Liu, Jing Chen, Zhimin Liu, Tiancheng Mu, Rui Zhang and Guangying Yang

Center for Molecular Sciences, Institute of Chemistry, Chinese Academy of Sciences, Beijing 100080, China. E-mail: Hanbx@iccas.ac.cn; Fax: 86-10-62562821; Tel: 86-10-62562821

Received 27th November 2003, Accepted 10th February 2004
First published as an Advance Article on the web 10th March 2004

FTIR and UV-vis techniques were used to investigate the effect of ultrasound on the microenvironment of sodium bis(2-ethylhexyl) sulfosuccinate (AOT) reverse micelles in *iso*-octane. The studies revealed that ultrasound resulted in re-aggregation of the reverse micelles and thus enlarged the water core of the micelles. On the basis of these investigations, ZnS nanorods and nanofibers were synthesized in the reverse micelles by the ultrasound-induced method. A possible mechanism for ultrasound-induced formation of nanorods and nanofibers in reverse micelles is discussed.

1 Introduction

The synthesis of nano-sized materials of specific size and shape has attracted much attention in various fields such as modern materials,[1–4] catalysis,[5–7] electronics,[8–10] biotechnology[11–13] and so on. Particularly, nanoparticles with high order structures (*e.g.*, nanorods, nanofibers and nanowires) have received more and more interest due to their potential applications in nanodevices.[14–16] The template method is very effective for the fabrication of nanostructures of desired materials. It can be classified into hard and soft template methods. The former, involves the use of carbon nanotubes,[17–20] porous alumina,[21–23] and nanochannel glass,[24,25] through which the size, shape and alignment of nanoparticles can be controlled. The latter, involves the use of various kinds of microemulsions and micelles. As the reaction is restricted in the micellar core, the growth of the nanoparticles can be controlled by the size and shape of the polar core.[26,27] In most cases, spherical nanoparticles are formed within the polar cores of reverse micelles. However, under some conditions, further growth and aggregation of the initially formed nanoparticles results in the formation of higher order structures such as needles,[28] fibers,[29] and wires.[30–32] This principle has been exemplified through a number of studies involving inorganic precipitation in bicontinuous microemulsions,[33–35] block copolymer micelles,[36–39] and other methods.[40,41]

In recent years, sonochemistry has become a rapidly growing research area. It is well known that ultrasonic radiation in liquids has a variety of physical and chemical effects deriving from acoustic cavitation, which can provide a unique method for driving chemical reactions under extreme conditions.[42] Some of the most important aspects of sonochemistry recently, are its applications in material chemistry. Diverse applications of ultrasound have been exploited in inorganic nanostructured materials synthesis,[43–45] biomaterials preparation (protein microspheres)[46,47] and sonochemical synthesis of polymers.[48–50] Some nanorods or nanowires of inorganic materials have been synthesized using sonochemical methods.[51–54]

Recently, we discovered that spherical silver nanoparticles in sodium bis(2-ethylhexyl) sulfosuccinate (AOT)/*iso*-octane reverse micelles could form nanofibers with the aid of ultrasound.[55] We also studied the effect of ultrasound on the microstructure of reverse micelles by SAXS, which showed that the micellar shape transformed from spherical to ellipsoidal with ultrasound.[55] In the present work, we continue the fundamental and application studies of this interesting topic. The effects of ultrasound on the microenvironment inside reverse micelles are investigated by FTIR and UV-vis techniques, and the possible induced formation of ZnS (a semiconductor) nanorods and nanofibers by ultrasound is explored. It is revealed that ultrasound results in the re-aggregation of the reverse micelles and thus enlarges the water core of the micelles. Spherical ZnS nanoparticles can also transform into nanorods and nanofibers in the reverse micelles with the aid of ultrasound, and their length can be controlled by ultrasound time.

2 Experimental

Materials

CO_2 ($>99.995\%$ purity) was provided by Beijing Analysis Instrument Factory. The surfactant AOT was purchased from Sigma with a purity of 99%. Methyl orange, *iso*-octane, Na_2S, $ZnSO_4$, and ethanol supplied by the Beijing Chemical Plant were all A. R. grade. Doubly-distilled water was used.

FTIR spectra of reverse micelles

The reverse micellar solution ([AOT] = 50 mmol L^{-1}) was prepared by dissolving AOT into *iso*-octane in a flask. The required amount of water was added to the surfactant solution to reach the desired *w* (molar ratio of water to AOT). The flask was shaken until a clear solution was obtained. The reverse micellar solution was treated in an ultrasonic cleaning bath (20 kHz) filled with water at 298.2 K for the desired time. FTIR spectra of the reverse micelles were recorded by a BRUKER spectrophotometer (Model TENSOR-27). Each sample was recorded with 32 scans at an effective resolution of 2 cm^{-1}.

UV-vis spectra of methyl orange in reverse micelles

The required amount of an aqueous solution of methyl orange was added to the AOT/*iso*-octane solution (50 mmol L^{-1}). The flask was shaken until a clear solution was obtained. The reverse micellar solution was treated in an ultrasonic cleaning bath (20 kHz) filled with water at 298.2 K for the

DOI: 10.1039/b315399a

desired time. UV-vis adsorption spectra were recorded using a TU-1201 Model spectrophotometer.

UV-vis spectra of ZnS nanoparticles in reverse micelles

The synthesis of zinc sulfide in reverse micelles was similar to that reported in the literature.[56] Briefly, reverse micellar solutions containing Na_2S (0.6 mol L^{-1}) and $ZnSO_4$ (0.6 mol L^{-1}) were first prepared by adding the corresponding salt solution to 50 mmol L^{-1} AOT/*iso*-octane solution to give the required w value. The two micellar solutions containing the reactants, respectively, were mixed and ZnS nanoparticles were formed in the reverse micelles. After the reverse micelles containing ZnS nanoparticles had been irradiated by ultrasound for a certain time (as discussed above), UV spectra were recorded using a TU-1201 Model spectrophotometer.

Recovery and characterization of ZnS nanoparticles

The reverse micellar solution with ZnS nanoparticles was loaded into a sealed flask and treated in an ultrasonic cleaning bath (20 kHz) filled with water at 298.2 K for the desired time. The solvent *iso*-octane was evaporated, and the deposits were washed repeatedly by ethanol and water to remove the surfactant and by-products. The morphologies of the obtained ZnS were determined by transmission electron microscopy (TEM) with an HITACHI H-600A electron microscope. Particles were dispersed in ethanol and then directly deposited on the copper grid. The X-ray diffractogram (XRD) was recorded by an X-ray diffractometer (XRD, Model D/MAX2500, Rigaka) with Cu Kα radiation.

3 Results and discussion

FTIR spectra of reverse micelles

The broad band of hydroxyl stretching [ν(O–H)] is usually used in detailed investigations of reverse micelles.[57–61] Fig. 1 shows the hydroxyl stretching vibration of the reverse micelles after different ultrasound times, and the C–H contribution to the O–H band has been removed by subtracting the spectrum of *iso*-octane. A large increase in the absorbance with increasing ultrasound time is observed. The total peak area of the O–H stretching band of water increases with the size of the water core.[57,59] Thus, the increased absorbance shown in Fig. 1 is an indication of the enlarged water core caused by ultrasound. The asymmetrical hydroxyl stretching band can be fitted to 4 Gaussion functions.[59] As examples, Fig. 2 shows the results with an ultrasound time of 0.5 h. The four peaks centered at 3610 ± 20, 3540 ± 20, 3420 ± 20, and 3230 ± 20 cm^{-1} are ascribed to four different states of the molecules, *i.e.* trapped water in the palisade layer of the reverse micelles, bound water with the sulfo group of AOT, free water, and bound water with sodium counterion, respectively.[59] Since the total peak area corresponding to the water band is the sum of the peak area of the different states of water, the mole fraction of each state of water can be calculated from the ratio of each subpeak area to the total peak area, and the results are shown in Fig. 3. It reveals that the mole fraction of the free water and the bound water with sodium counterion increases with increasing ultrasound time, while the mole fractions for the other two bands decrease. The increased mole fraction of free water also indicates the enlargement of water core in the micelles. With the enlarged water core, the dissociation degree of the polar head-group of AOT molecules increases, which makes the mole ratio of bound water with sodium counterion increase.[59]

The changes of the carbonyl stretching vibration [ν(C=O)] also provide information on the microenvironment change of reverse micelles caused by ultrasound, which is shown in Fig. 4. As shown in the figure the intensity is enhanced by ultrasound. The broad peak with an asymmetric shape shown in Fig. 4 suggests that the band is a fusion of the peaks corresponding to carbonyl groups in different microenvironments.[57,62] The Gaussian curve fitting program was also used to treat the peaks, by which two peaks centered at 1740 ± 2 cm^{-1} and 1721 ± 2 cm^{-1} were obtained. Their intensity ratio ($I_r = I_{1740}/I_{1721}$) is closely related to the polarity of the water core, *i.e.* the ratio decreases in a more polar environment because more conformations change from *gauche* to *trans*.[62,63] The intensity ratios ($I_r = I_{1740}/I_{1721}$) as a function of ultrasound time are given in the inset of Fig. 4. As can be seen, the ratio decreases gradually with increasing ultrasound time. Thus, the decreased ratio of the *trans* and *gauche* configurations

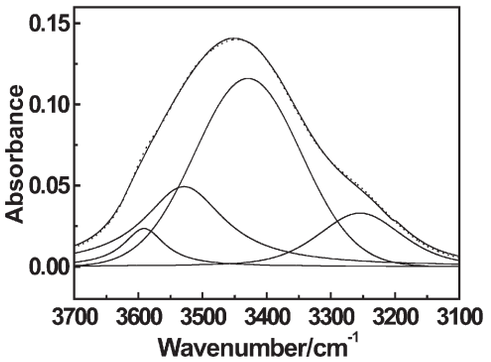

Fig. 2 Deconvoluted hydroxyl stretching vibration of water in reverse micelles ([AOT] = 50 mmol L^{-1}, $w = 10$) at 298.2 K after ultrasound for 0.5 h.

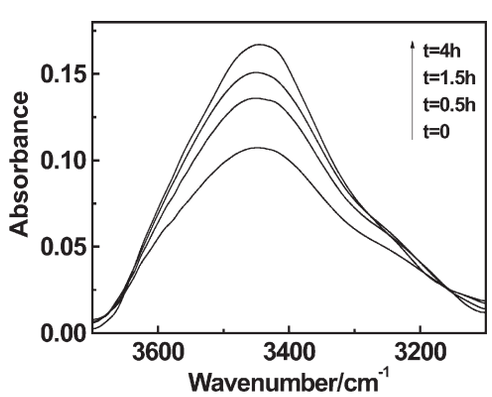

Fig. 1 IR spectra of the hydroxyl stretching vibration of water in AOT reverse micelles ([AOT] = 50 mmol L^{-1}, $w = 10$) at 298.2 K after different ultrasound times (t).

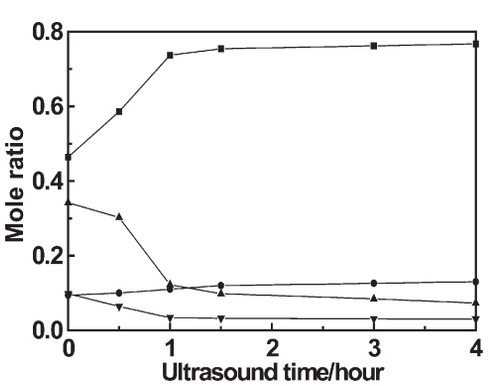

Fig. 3 Variation of molar ratio of four states of water in reverse micelles with ultrasound time (■ the free water, ● the bound water with sodium counterion, ▲ the bound water with the sulfo group of AOT, ▼ trapped water in the palisade layer of reverse micelles).

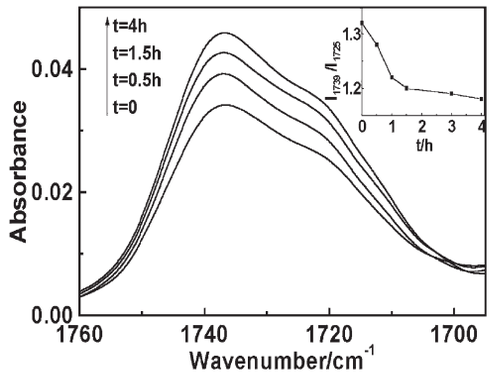

Fig. 4 IR spectra of the carbonyl stretching vibration of reverse micelles (AOT = 50 mmol L^{-1}, $w = 10$) at 298.2 K after different ultrasound times (t). The inset shows the variation of intensity ratio ($I_r = I_{1740}/I_{1721}$) as a function of ultrasound time.

with ultrasound time also provides information on the enlarged polar region of micellar cores. The enhanced polarity causes more polar groups directed towards the polar side of the interface, *i.e.* the configurations transfer from *trans* to *gauche*.

UV-vis spectra of methyl orange in reverse micelles

Methyl orange (MO) can be used as a solvatochromic micropolarity probe since its absorption spectrum is sensitive to

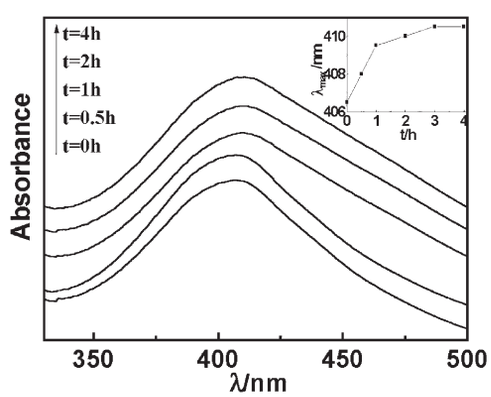

Fig. 5 UV absorption of methyl orange in reverse micelles ([AOT] = 50 mmol L^{-1}, $w = 10$) after different ultrasound times (t). The inset shows the variation of λ_{max} as a function of ultrasound time.

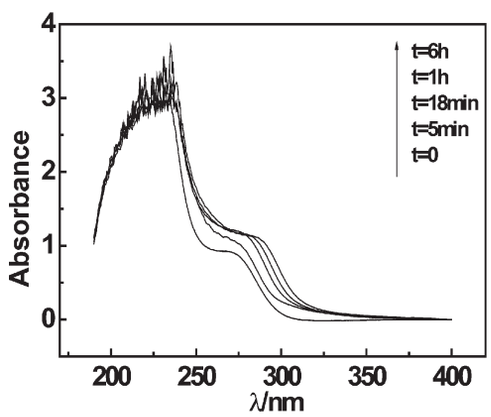

Fig. 6 UV spectra of reverse micelles ([AOT] = 50 mmol L^{-1}, $w = 10$, [ZnS] = 1.2 mmol L^{-1}) containing ZnS for various ultrasound times (t).

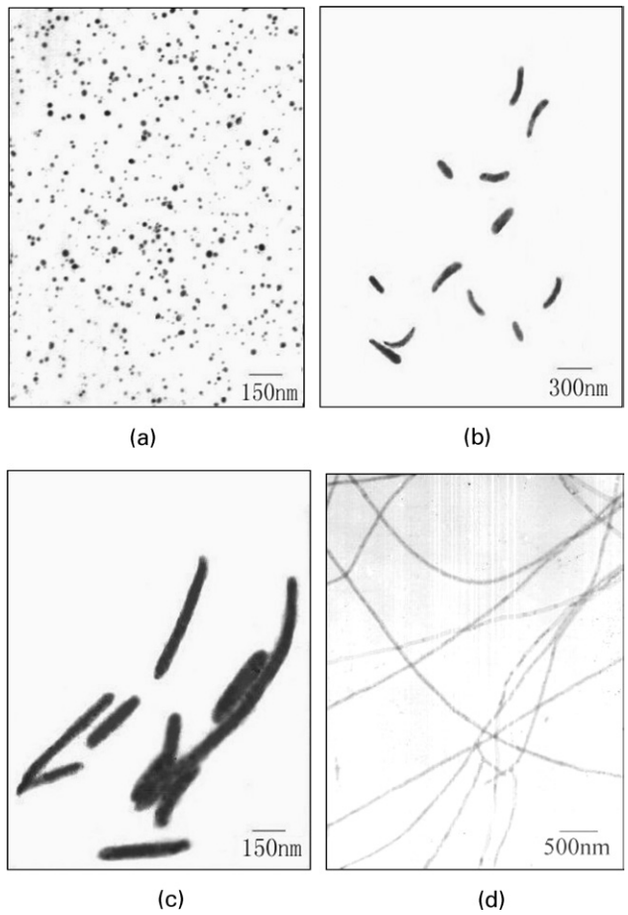

Fig. 7 TEM photographs of ZnS particles with different ultrasound times (t). (a) $t = 0$; (b) $t = 0.5$ h; (c) $t = 2$ h; (d) $t = 4$ h.

medium effects.[64–66] The long wavelength absorption band of MO shifts to shorter wavelengths upon decreasing the polarity of the medium in which the probe exists. This property also makes MO useful for reporting the ultrasound-induced environmental changes in the reverse micelles. The variation in the absorption spectra of MO with ultrasound time is shown in Fig. 5. It is obvious that the absorbance of MO red shifts gradually with increasing ultrasound time, which indicates that the water in micellar cores is more like bulk water. This is consistent with the enlarged water core of micelles induced by ultrasound. The results obtained from UV-vis spectra agreed well with those obtained from FTIR spectra.

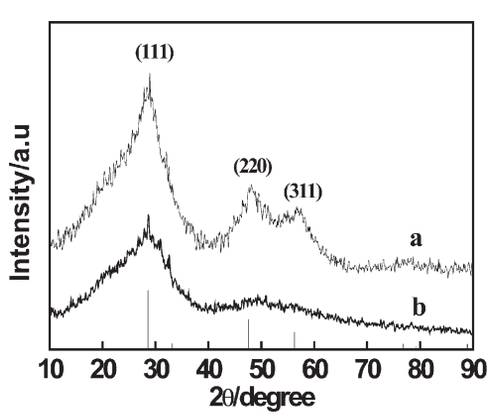

Fig. 8 XRD patterns of ZnS obtained by ultrasound for 0.5 h (a) and without ultrasound (b). The vertical lines at the bottom indicate the standard position and relative intensities of cubic ZnS.

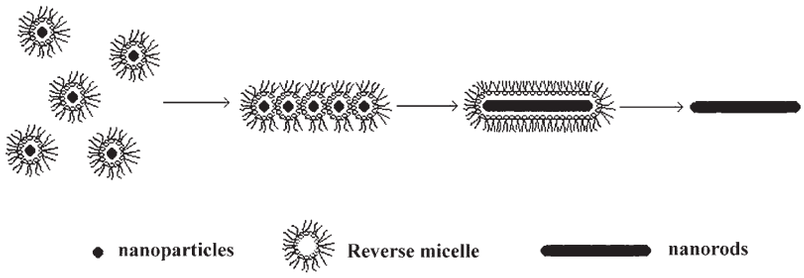

Fig. 9 Proposed mechanism for the ultrasound-induced formation of nanorods and nanofibers in AOT reverse micelles.

UV-vis spectra of ZnS nanoparticles in reverse micelles

UV-vis spectrum is a useful technique for *in-situ* characterization of semiconductor nanoparticles in reverse micelles.[67–70] Fig. 6 illustrates some representative UV-vis adsorption spectra of ZnS nanoparticles dispersed in reverse micelles ($w = 10$, [AOT] = 50 mmol L^{-1}) as a function of ultrasound time. The bands at about 275 nm and 225 nm are attributed to the absorption of ZnS nanoparticles and the surfactant AOT, respectively. It is observed that with ultrasound irradiation, the absorption band of ZnS is largely red-shifted with increased intensity. It is well known that, as a consequence of quantum confinement of the photogenerated electron-hole pair, the UV-vis absorption spectrum of semiconductor nanoparticles depends on their size, *i.e.*, the wavelength at the maximum absorption (λ_{max}) increases as the nanoparticle size increases.[56,71] The large red shift of λ_{max} by ultrasound suggests an increased size of ZnS nanoparticles in the reverse micelles. In addition, as we know, the maximum and the bandwidth of the absorption band depend on the surrounding medium of the particles. The microstructure of the reverse micelles should change with the aggregation of ZnS nanoparticles because the nanoparticles are confined in the micellar cores. This may contribute partially to the change of the ZnS adsorption band.

Formation of ZnS nanorods and nanofibers

All of the above spectroscopic investigations show that the microenvironment of the reverse micelles are enlarged by ultrasound. We applied this concept to the synthesis of ZnS nanoparticles, and the morphologies of the obtained ZnS are shown in Fig. 7. Without ultrasonic treatment, only spherical nanoparticles with diameters of 10–25 nm were obtained (see Fig. 7a). However, ZnS nanorods or nanofibers were formed after the micellar solution was treated with ultrasonic radiation, which are shown in Fig. 7b–d. It is evident that the length of the nanorod is increased with increasing ultrasound time. Given enough time for ultrasonic radiation ($t = 4$ h), wire-like nanoparticles of ZnS with diameters of about 50 nm and lengths of 10 μm were obtained (Fig. 7d). The XRD patterns of the ZnS prepared with and without ultrasound irradiation are shown in Fig. 8a and 8b, respectively. Fig. 8a shows the presence of broad peaks corresponding to nanocrystals, of which the three strong diffraction peaks correspond to 111, 220, and 311 planes of the cubic crystalline ZnS (JCPDS No. 5-566). On comparison with Fig. 8b, it is evident that the degree of dispersion of the peaks after ultrasound treatment is lower, indicating the larger size of ZnS particles, which is consistent with the TEM results. From Fig. 8, it is also known that ultrasound cannot change the crystal phase of ZnS nanoparticles synthesized in reverse micelles.

Proposed mechanism for the formation of nanofibers

In previous work, we have studied the effect of ultrasound on the microstructure of reverse micelles using small-angle X-ray scattering.[55] It is revealed that the shape of the micelles change from spherical to ellipsoidal after treatment by ultrasound. In conjunction with the results obtained from this work, it can be deduced that ultrasound induces the shape change accompanied by re-aggregation of the micelles. Based on the above investigations, we propose a possible mechanism for the formation of nanorods and nanofibers induced by ultrasound, which is schematically shown in Fig. 9. Introduction of ultrasound to the micellar solution can result in re-assembly of reverse micelles, the original spherical micelles fusing end-to-end to form cylindrical structures, which is coupled with aggregation of nanoparticles dispersed in reverse micelles. It is expected that, the re-assembly of the surfactants caused by ultrasound induces the aggregation of ZnS particles in reverse micelles, which in turn affects the re-assembly of the surfactants. Namely, the re-assembly of the surfactants and the aggregation of ZnS particles confined in the micellar cores can promote each other.

4 Conclusion

FTIR and UV-vis spectra provide direct information on the microenvironmental changes of AOT reverse micelles induced by ultrasound. It is revealed that ultrasound can enlarge the water core and polar region of the reverse micelles, which result from re-assembly of the reverse micelles. Using this concept, ZnS nanorods and nanofibers have been successfully prepared in the reverse micelles by the ultrasound-induced method. This method is simple and versatile, and can be easily applied to the synthesis of nanorods and nanofibers of many other materials.

Acknowledgements

The authors are grateful to the National Natural Science Foundation of China (20133030, 20374057).

References

1 M. Moreno-Manas, R. Pleixats and S. Villarroya, *Chem. Commun.*, 2002, 60.
2 B. I. Lemon and R. M. Crooks, *J. Am. Chem. Soc.*, 2000, **122**, 12 886.
3 Y. M. Li, W. Kim, Y. G. Zhang, M. Rolandi, D. W. Wang and H. J. Dai, *J. Phys. Chem. B*, 2001, **105**, 11 424.
4 I. G. Loscertales, A. Barrero, I. Guerrero, R. Cortijo, M. Marquez and A. M. Ganan-Calvo, *Science*, 2002, **295**, 1695.
5 H. Ohde, C. M. Wai, H. Kim, J. Kim and M. Ohde, *J. Am. Chem. Soc.*, 2002, **124**, 4540.
6 L. K. Yeung, C. T. Lee, K. P. Johnston and R. M. Crooks, *Chem. Commun.*, 2001, 2290.
7 T. K. Sau, A. Pal and T. Pal, *J. Phys. Chem. B*, 2001, **105**, 9266.
8 W. P. Wuelfing, S. J. Green, J. J. Pietron, D. E. Cliffel and R. W. Murray, *J. Am. Chem. Soc.*, 2000, **122**, 11 465.
9 T. Trindade, P. O'Brien and N. L. Pickett, *Chem. Mater.*, 2001, **13**, 3843.

10 P. Poizot, S. Laruelle, S. Grugeon, L. Dupont and J. M. Tarascon, *Nature*, 2000, **407**, 496.
11 N. Kurth, E. Renard, F. Brachet, D. Robic, P. Guerin and R. Bourbouze, *Polymer*, 2002, **43**, 1095.
12 C. M. Niemeyer, *Angew. Chem., Int. Ed.*, 2001, **40**, 4128.
13 F. Caruso and C. Schuler, *Langmuir*, 2000, **16**, 9595.
14 J. Muster, G. T. Kim, V. Krstic, J. G. Park, Y. W. Park, S. Roth and M. Burghard, *Adv. Mater.*, 2000, **12**, 420.
15 X. F. Duan and C. M. Lieber, *J. Am. Chem. Soc.*, 2000, **122**, 188.
16 Z. W. Pan, Z. R. Dai and Z. L. Wang, *Science*, 2001, **291**, 1947.
17 Y. Huang, X. F. Duan, Y. Cui, L. J. Lauhon, K. H. Kim and C. M. Lieber, *Science*, 2001, **294**, 1313.
18 K. Matsui, B. K. Pradhan, T. Kyotani and A. Tomita, *J. Phys. Chem. B*, 2001, **105**, 5682.
19 S. Fullam, D. Cottell, H. Rensmo and D. Fitzmaurice, *Adv. Mater.*, 2000, **12**, 1430.
20 A. Govindaraj, B. C. Satishkumar, M. Nath and C. N. R. Rao, *Chem. Mater.*, 2000, **12**, 202.
21 H. Q. Cao, Y. Xu, J. M. Hong, H. B. Liu, G. Yin, B. L. Li, C. Y. Tie and Z. Xu, *Adv. Mater.*, 2001, **13**, 1393.
22 H. Q. Cao, Z. Xu, X. W. Wei, X. Ma and Z. L. Xue, *Chem. Commun.*, 2001, 541.
23 K. Nielsch, F. Muller, A. P. Li and U. Gosele, *Adv. Mater.*, 2000, **12**, 582.
24 P. P. Nguyen, D. H. Pearson, R. J. Tonucci and K. Babcock, *J. Electrochem. Soc.*, 1998, **145**, 247.
25 A. D. Berry, R. J. Tonucci and M. Fatemi, *Appl. Phys. Lett.*, 1996, **69**, 2846.
26 B. A. Simmons, S. C. Li, V. T. John, G. L. McPherson, A. Bose, W. L. Zhou and J. B. He, *Nano Lett.*, 2002, **2**, 263.
27 A. Meziani, D. Touraud, A. Zradba, S. Pulvin, I. Pezron, M. Clausse and W. Kunz, *J. Phys. Chem. B*, 1997, **101**, 3620.
28 G. B. Khomutov, *Colloid Surf., A*, 2002, **202**, 243.
29 M. Li and S. Mann, *Langmuir*, 2000, **16**, 7088.
30 J. K. Lee, W. K. Koh, W. S. Chae and Y. R. Kim, *Chem. Commun.*, 2002, 138.
31 G. D. Rees, R. Evans-Gowing, S. J. Hammond and B. H. Robinson, *Langmuir*, 1999, **15**, 1.
32 L. M. Qi, J. M. Ma, H. M. Cheng and Z. G. Zhao, *J. Phys. Chem. B*, 1997, **101**, 3460.
33 J. Liu, W. K. Teo, C. H. Chew and L. M. Gan, *J. Appl. Polym. Sci.*, 2000, **77**, 2785.
34 C. H. Chew, T. D. Li, L. H. Gan, C. H. Quek and L. M. Gan, *Langmuir*, 1998, **14**, 6068.
35 K. Aikawa, K. Kaneko, T. Tamura, M. Fujitsu and K. Ohbu, *Colloid Surf., A*, 1999, **150**, 95.
36 H. Y. Zhao and E. P. Douglas, *Chem. Mater.*, 2002, **14**, 1418.
37 T. B. Liu, Y. Xie and B. Chu, *Langmuir*, 2000, **16**, 9015.
38 V. M. Cepak and C. R. Martin, *J. Phys. Chem. B*, 1998, **102**, 9985.
39 C. W. Chen, M. Q. Chen, T. Serizawa and M. Akashi, *Adv. Mater.*, 1998, **10**, 1122.
40 C. Y. Wang, M. H. Chen, G. M. Zhu and Z. G. Lin, *J. Colloid Interface Sci.*, 2001, **243**, 362.
41 S. D. Wu, Z. G. Zhu, J. Y. Tan and J. C. Gao, *Chem. Lett.*, 2001, **5**, 396.
42 K. S. Suslick and G. J. Price, *Annu. Rev. Mater. Sci.*, 1999, **29**, 295.
43 P. Cintas and J. L. Luche, *Green Chem.*, 1999, **1**, 115.
44 O. A. C. Nunes, Q. Fanyao, W. Santos, A. L. Fonseca and D. Agrello, *J. Appl. Phys.*, 1998, **84**, 2420.
45 K. V. P. M. Shafi, A. Ulman, A. Dyal, X. Z. Yan, N. L. Yang, C. Estournes, L. Fournes, A. Wattiaux, H. White and M. Rafailovich, *Chem. Mater.*, 2002, **14**, 1778.
46 R. Langer, *Acc. Chem. Res.*, 2000, **33**, 94.
47 L. L. Johnson, R. V. Peterson and W. G. Pitt, *J. Biomater. Sci., Polym. Ed.*, 1998, **9**, 1177.
48 R. C. Hiorns, A. Khoukh, P. Ghigo, S. Prim and J. Francois, *Polymer*, 2002, **43**, 3365.
49 H. Kim and J. W. Lee, *Polymer*, 2002, **43**, 2585.
50 Y. Q. Liao, Q. Wang, H. S. Xia, X. Xu, S. M. Baxter, R. V. Slone, S. G. Wu, G. Swift and D. G. Westmoreland, *J. Polym. Sci., Part A: Polym. Chem.*, 2001, **39**, 3356.
51 H. Wang, J. J. Zhu, J. M. Zhu and H. Y. Chen, *J. Phys. Chem. B*, 2002, **106**, 3848.
52 R. V. Kumar, Y. Koltypin, X. N. Xu, Y. Yeshurun, A. Gedanken and I. Felner, *J. Appl. Phys.*, 2001, **89**, 6324.
53 Y. Koltypin, S. I. Nikitenko and A. Gedanken, *J. Mater. Chem.*, 2002, **12**, 1107.
54 S. I. Nikitenko, Y. Koltypin, Y. Mastai, M. Koltypin and A. Gedanken, *J. Mater. Chem.*, 2002, **12**, 1450.
55 J. L. Zhang, B. X. Han, M. H. Liu, D. X. Liu, Z. X. Dong, J. Liu, D. Li, J. Wang, B. Z. Dong, H. Zhao and L. X. Rong, *J. Phys. Chem. B*, 2003, **107**, 3679.
56 P. Calandra, M. Goffedi and V. T. Liveri, *Colloid Surf., A*, 1999, **160**, 9.
57 T. K. Jain, M. Varshney and A. Maitra, *J. Phys. Chem.*, 1989, **93**, 7409.
58 M. B. Temsamani, M. Maeck, I. EI Hassani and H. D. Hurwitz, *J. Phys. Chem. B*, 1998, **102**, 3335.
59 G. W. Zhou, G. Z. Li, A. J. Lou, W. J. Chen and M. Bao, *Sci. China, Ser. B*, 2001, **44**, 398.
60 P. D. Moran, G. A. Bowmaker, R. P. Cooney, J. R. Bartlett and J. L. Woolfrey, *Langmuir*, 1995, **11**, 738.
61 Y. Ikushima, N. Saito and M. Arai, *J. Colloid Interface Sci.*, 1997, **186**, 254.
62 G. W. Zhou, G. Z. Li, W. J. Chen, A. J. Lou and M. Bao, *Sci. China, Ser. B*, 2002, **45**, 68.
63 Q. Li, W. H. Li, S. P. Weng, J. G. Wu and G. X. Xu, *Wuli Huaxue Xuebao*, 1997, **13**, 438.
64 R. T. Buwalda and J. B. F. N. Engberts, *Langmuir*, 2001, **17**, 1054.
65 C. B. Roberts and J. B. Thompson, *J. Phys. Chem. B*, 1998, **102**, 9074.
66 B. Geetha, A. B. Mandal and T. Ramasami, *Macromolecules*, 1993, **26**, 4083.
67 C. Petit, P. Lixon and M. P. Pileni, *J. Phys. Chem.*, 1993, **97**, 12 974.
68 J. A. Greighton and D. G. Eaton, *J. Chem. Soc., Faraday Trans.*, 1991, **87**, 3881.
69 J. P. Cason, K. Khambaswadkar and C. B. Roberts, *Ind. Eng. Chem. Res.*, 2000, **39**, 4749.
70 M. Ji, X. Chen, C. M. Wai and J. L. Fulton, *J. Am. Chem. Soc.*, 1999, **121**, 2631.
71 N. Yasuhiro and N. Yoshio, *Langmuir*, 1997, **13**, 4295.